Biochemistry and Biophysics Reports 42 (2025) 101967

Contents lists available at ScienceDirect

Biochemistry and Biophysics Reports

journal homepage: www.elsevier.com/locate/bbrep

Alterations of renal polyamine metabolism in mice with folic acid-induced chronic kidney disease

Cheng Xue [a,1], Jiaxin Chen [a,1], Xinming Li [a], Chenchen Zhou [a,b], Zhiguo Mao [a,*]

[a] Division of Nephrology, Shanghai Changzheng Hospital, Naval Medical University (Second Military Medical University), Shanghai, China
[b] Outpatient Department, Yangpu Third Military Retreat, Yangpu first retirement, Shanghai, 200000, China

ARTICLE INFO

Keywords:
Mass spectrometry imaging
Metabolomic
Chronic kidney disease

ABSTRACT

Chronic kidney disease (CKD) often follows acute kidney injury, leading to renal fibrosis and progressive renal failure. Spermine, a polyamine with antioxidant and anti-inflammatory properties, helps reduce renal fibrosis and may serve as a biomarker for CKD progression. We used spatially resolved metabonomic analysis with AFADESI-MSI to examine polyamine distribution in kidneys of a folic acid (FA)-induced CKD mouse model. Results showed decreased spermine and increased spermidine levels, associated with elevated spermine oxidase (SMOX) and spermidine/spermine N1-acetyltransferase (SSAT) enzyme expression in CKD. These findings suggest that altered polyamine metabolism contributes to CKD progression and may provide targets for polyamine-based therapies.

1. Introduction

Chronic kidney disease (CKD) is a significant global health concern, often emerging as a consequence of unresolved kidney damage following acute kidney injury (AKI) [1]. CKD is characterized by sustained kidney damage that leads to structural and functional changes in the kidneys, including renal fibrosis, which severely impairs kidney function and can contribute to long-term renal failure.

Polyamines, particularly spermine, play a crucial role in regulating cell growth, differentiation, and survival [2]. In CKD, spermine is particularly significant due to its antioxidant and anti-inflammatory properties, which help mitigate renal fibrosis and reduce kidney damage [3]. Additionally, spermine holds potential as a biomarker for CKD progression and therapeutic response, providing a valuable tool for early diagnosis and monitoring treatment efficacy [4].

However, the precise localization of polyamine expression in kidneys remains unclear, prompting further investigation. To address gaps identified in the original study, we conducted spatially resolved metabonomic analysis based on air flow-assisted desorption electrospray ionization (AFADESI) integrated mass spectrometry imaging (MSI) to examine the distribution of polyamine metabolites, including spermine and spermidine, in the kidneys of a model of folic acid (FA) induced CKD after AKI.

2. Methods

2.1. Chemicals and reagents

FA was obtained from Meilunbio (Dalian, China). Trizol, reverse transcript reagents, and SYBR Green RT-qPCR Kit were acquired from Takara (Otsu, Japan). MS-grade acetonitrile and positive charge desorption plates were purchased from Thermo Fisher (USA). The AFADESI-MSI platform was developed by Beijing Victor Technology Co. LTD (Beijing, China). The 7900HT Real-Time PCR System was obtained from Applied Biosystems (Waltham, MA). A frozen slicer was used from Leica CM 1950 (Germany).

2.2. Animals

This study used an FA-induced CKD model in C57BL/6J mice following AKI (14 days after FA injection, 5 male mice in each group) to investigate the spatial distribution of polyamines in the kidney. Mice

* Corresponding author. Division of Nephrology, Shanghai Changzheng Hospital, Second Affiliated Hospital of Naval Medical University (Second Military Medical University), 415 Fengyang Road, Shanghai, 200003, China.
E-mail addresses: chengxia1568@126.com (C. Xue), chenjiaxin246@126.com (J. Chen), maozhiguo518@126.com, maozhiguo93@126.com, maozhiguo@smmu.edu.cn (Z. Mao).
[1] Equal contributors.

https://doi.org/10.1016/j.bbrep.2025.101967
Received 16 November 2024; Received in revised form 6 February 2025; Accepted 26 February 2025
2405-5808/© 2025 The Authors. Published by Elsevier B.V. This is an open access article under the CC BY-NC license (http://creativecommons.org/licenses/by-nc/4.0/).

were divided into FA-treated and control groups, and kidney tissues were analyzed using histological staining, AFADESI-MSI, and biochemical assays to assess changes in polyamine metabolism. 8-week old male C57BL/6J mice (stock no:000664) were used from JAX Laboratory (USA). To construct the renal injury model, FA groups were intraperitoneally administered folic acid in a 0.3 M NaHCO3 vehicle (250 mg/kg), while the control group received only the NaHCO3 vehicle. All mice were euthanized 14 days after injection. Mice were anesthetized with isoflurane inhalation to collect blood from the eyeball and then euthanized by cervical dislocation. Kidneys were collected for biochemical, histopathological, and metabolic enzyme analysis.

All animal experiments complied with the ARRIVE guidelines and were conducted following the Guidance on the Operation of the Animals (Scientific Procedures) Act 1986 and associated guidelines. The study protocols were approved by the Animal Care and Use Committee of the Second Military Medical University (approval number: CZ240619). The influence of sex on the study results was not assessed, as only male mice were used.

2.3. Biochemical analysis and histological staining

Blood samples were collected and stored overnight at 4 °C. Serum was separated by centrifugation at 3000 rpm for 10 min, and biochemical parameters, including blood urea nitrogen (BUN) and serum creatinine (SCR), were measured using an automatic chemistry analyzer. Kidneys from three mice in each group were stained with hematoxylin-eosin (H&E) and Masson's trichrome to evaluate histopathological lesions and fibrosis.

2.4. AFADESI-MSI analysis of renal sections

The right kidneys of 6 male mice (3 from each group) were cut in half. One half was embedded in Cryo-Gel for spatial metabonomic analysis. Excess fluid was carefully absorbed with filter paper before embedding. Embedded kidneys were quickly frozen on dry ice for 30 min and stored at −80 °C until further analysis. Kidneys were sectioned into continuous sagittal sections of about 10 μm using a frozen slicer and thaw-mounted on a positive charge desorption plate. Three adjacent frozen sections were selected for AFADESI analysis in both positive and negative ion modes, along with H&E staining. The AFADESI-MSI platform (Beijing Victor Technology Co., LTD., Beijing, China) and Q-Orbitrap mass spectrometer (Q Exactive, Thermo Scientific, U.S.A) were used for MSI analysis in positive and negative ion modes. The solvent used was ACN/H2O (8:2) for negative mode and ACN/H2O (8:2, 0.1 % formic acid) for positive mode, with a flow rate of 5 μL/min. The transfer gas flow rate was 45 L/min, the spray voltage was 7 kV, and the distance between the sample surface, sprayer, and ion transport tube was 3 mm. MS resolution was set at 70,000, mass ranges 70–1000 Da, AGC target 2E6, maximum injection time 200 ms, S-lens voltage 55 V, and capillary temperature 350 °C. MSI scanning was performed at 200 μm/s in the X direction and a vertical step of 100 μm in the Y direction.

2.5. Data processing and analysis

ImzMLConverter was used to convert the raw mass spectrometry files to ".IMZML" format, which were then imported into MSiReader for ion image reconstruction after background subtraction using Cardinal software. All mass spectrometry images were normalized using total ion number normalization per pixel. Metabolites with VIP values > 1.0 and P-values < 0.05 were considered significant. Annotation of metabolites was performed using the SmetDB database and the pySM annotation framework.

2.6. RNA extraction and Real-Time PCR

Total RNA was extracted from samples using TRIzol, and cDNA was synthesized using reverse transcript reagents. Real-time PCR was conducted using the SYBR Green RT-qPCR Kit and a 7900HT Real-Time PCR System. Relative gene expression levels were calculated using the $2^{\Delta\Delta CT}$ method with GAPDH as control (Table 1).

2.7. Western blotting

Tissue or cell lysates were prepared using RIPA buffer containing 50 mM Tris-HCl, 1 mM EDTA, 150 mM NaCl, 1 % Triton, and 2 % SDS, along with phosphatase and protease inhibitors. The lysates were clarified by centrifugation. Equivalent protein amounts were loaded onto SDS-PAGE gels and then transferred onto polyvinylidene difluoride (PVDF) membranes. Membranes were blocked with 3 % BSA and incubated with primary antibodies, followed by incubation with suitable secondary antibodies. Enhanced chemiluminescence reagent was used for signal detection. Primary antibodies included SMOX (1:1000, 15052-1-AP) and SAT1 (1:1000, #DF12469).

2.8. Statistical analysis

Statistical analysis was performed using GraphPad Prism 9.5. Comparisons between groups were conducted using two-tailed t-tests for normally distributed data and Wilcoxon tests for skewed data. Results are presented as mean ± SD, $P < 0.05$ indicated statistical significance.

3. Results

H&E staining showed a substantial infiltration of inflammatory cells in the renal interstitium of FA-treated mice compared to control mice. Masson staining revealed pronounced renal fibrosis in FA-treated mice (Fig. 1A). Furthermore, FA treatment significantly elevated blood urea nitrogen (BUN) and serum creatinine (SCR) levels compared to control mice (Fig. 1B). A total of 724 metabolites were identified by AFADESI-MSI (Supplement 1). In comparing the CKD group with the Control group, a total of 89 and 95 differentially expressed metabolites (DEMs) were identified in the renal cortex and medulla, respectively. Among these DEMs, spermine and spermidine stood out as particularly noteworthy. In normal mice kidneys, spermine expression was higher in the medulla than in the cortex, whereas spermidine expression was higher in the cortex than in the medulla (Fig. 1C–Supplement 2). However, in the kidneys of CKD mice, these patterns are altered. Our findings indicated significant changes in these metabolites during FA-induced renal fibrosis. Specifically, the intensity of spermine was significantly lower, resulting in reduced expression in both the cortex and medulla, while spermidine levels were significantly higher, with a more significant increase in the cortex (Fig. 1D). Fig. 1E illustrates that spermine/spermine N1 acetyltransferase (SSAT) and SMOX are key enzymes involved in the conversion of polyamines. SSAT, encoded by SAT1, primarily catalyzes the acetylation of spermine and spermidine, whereas SMOX directly oxidizes and decomposes spermine into spermidine without acetylation. Western blotting and RT-PCR results confirmed that the expressions of SMOX and SAT1 were both significantly elevated in FA-treated mice compared to controls (Fig. 1F and G).

4. Discussion

Our study reveals significant alterations in renal polyamine metabolism in mice with FA-induced CKD after AKI, providing new insights

Table 1
Mouse primer sequences for real-time PCR.

Primer	Forward	Reverse
Gapdh	GTCTTCACCACCATGGAGAAGG	CTAAGCAGTTGGTGGTGCAGGA
Smox	TGGCCTGTAGTCGTGGAGT	GCATGGCCTAAAGAAACTGGTG
Sat1	GAGAACACCCCTTCTACCACT	GCCTCTGTAATCACTCATCACGA

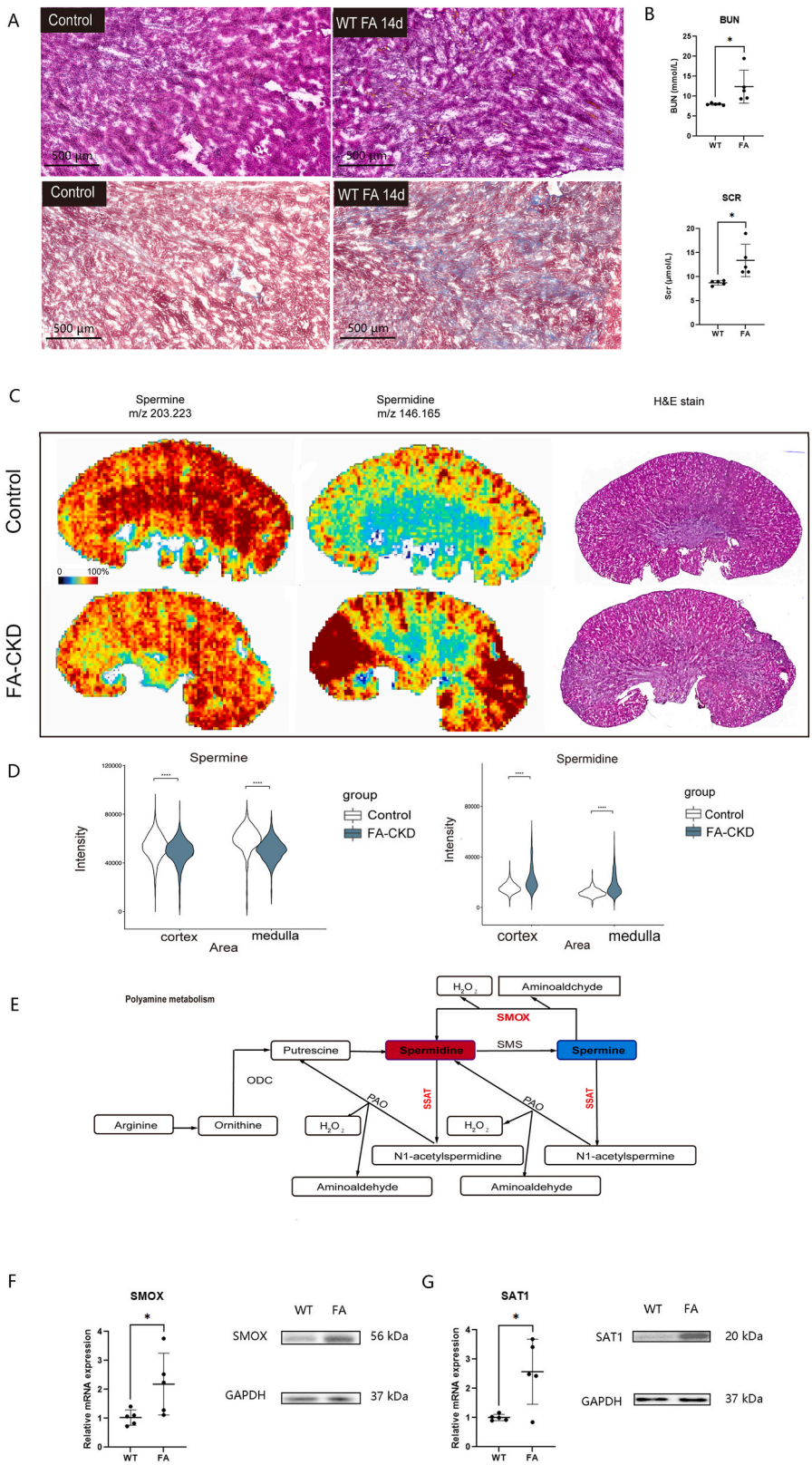

Fig. 1. Changes in polyamine metabolism in FA-treated mice and control mice. (A). H&E staining (up) and Masson staining (down). (B). Serum BUN and SCR levels. (C). Mass spectrometry imaging of spermine and spermidine in kidneys of control and FA-treated mice. (D). Boxplots of the intensity of spermine and spermidine in the cortex and medulla. (E). Polyamine metabolism process. SMOX, spermine oxidase; SAT1, spermidine/spermine N (1)-acetyltransferase 1. (F, G). MRNA and protein expression of SMOX and SAT in kidneys of control and FA-treated CKD mice (means ± SD). $^{*}P < 0.05$; $P < 0.00001$.

into the spatial dynamics of polyamine distribution in CKD. In normal kidneys, spermine and spermidine showed distinct spatial distribution patterns, with higher spermine levels in the medulla and increased spermidine in the cortex. However, these patterns were significantly disrupted in CKD after AKI, where spermine levels were reduced, and spermidine levels were increased. This shift in polyamine distribution suggests a potential disruption in polyamine homeostasis during CKD after AKI, which may contribute to renal damage and fibrosis.

Polyamines, especially spermine, are known for their protective roles in the kidney due to their antioxidant and anti-inflammatory properties [5]. Spermine can scavenge reactive oxygen species (ROS) and inhibit pro-inflammatory pathways, which are critical processes in preventing fibrosis and tissue damage. The depletion of spermine observed in our model could, therefore, exacerbate kidney injury, promoting fibrosis and compromising renal function. This is consistent with previous studies showing that reduced spermine levels are associated with increased oxidative stress and inflammation in CKD. Recent research has underscored the significance of the SMOX/spermine axis in CKD. In fibrotic kidneys, there is a marked increase in SMOX expression, leading to a significant reduction in spermine levels [6]. Exogenous spermine or genetic reduction of SMOX improves autophagy, reduces cellular senescence, and alleviates fibrosis in mice models [4].

The distinct distribution of spermine and spermidine in kidneys may be influenced by the different physiological roles of the cortex and medulla [7]. The cortex, which contains glomeruli and proximal tubules involved in filtration and reabsorption, has higher spermidine levels to support cell proliferation and high metabolic activity. In contrast, the medulla, prone to oxidative stress due to its hypoxic environment and ion transport functions, has higher spermine levels to provide antioxidant protection. The differential activity of key enzymes, such as SMOX and SSAT, also contributes to this distribution, reflecting the specific metabolic demands of each kidney region. This differential distribution of spermine and spermidine reflects the kidneys' need to adapt polyamine metabolism to local functional and environmental conditions, ensuring optimal protection and performance of renal tissues.

Our data demonstrated elevated expression of SMOX and SSAT in mice with CKD after AKI, further implicating these enzymes in the dysregulation of polyamine metabolism during renal injury. SMOX catalyzes the oxidation of spermine to spermidine, producing hydrogen peroxide as a byproduct, which can exacerbate oxidative stress and tissue damage [8]. Increased SMOX activity has been linked to kidney fibrosis and the progression of CKD, underscoring its role in disease pathogenesis. However, the upregulation of SSAT, which acetylates spermine and spermidine, primarily generates acetylated polyamines rather than fully degrading them [9]. Since SSAT-mediated acetylation does not effectively keep pace with the conversion and breakdown of spermidine, the overall spermidine levels remain elevated despite the increased enzyme activity, further contributing to the altered polyamine balance in renal injury.

Several limitations should be acknowledged. Our study used C57BL/6J mice, which carry a nicotinamide nucleotide transhydrogenase (NNT) mutation affecting mitochondrial redox balance. Since NNT deficiency increases oxidative stress, it may influence spermine depletion and SMOX upregulation. Future studies should validate these findings in C57BL/6 N mice, which have an intact NNT gene, to determine whether the observed polyamine alterations are primarily driven by CKD pathology or strain-specific redox differences. Second, although we demonstrated significant changes in spermine and spermidine levels, as well as upregulation of SMOX and SAT1, we did not directly assess whether targeted interventions that restore spermine levels or inhibit SMOX activity could mitigate renal fibrosis. Future research should explore potential therapeutic strategies, such as exogenous spermine supplementation to evaluate its renoprotective effects, SMOX inhibitors (e.g., MDL 72527), or genetic models to determine whether reducing spermine oxidation mitigates oxidative stress and fibrosis, and SAT1 modulation to better understand its role in polyamine homeostasis and renal injury progression [10]. Additionally, while our FA-induced CKD model mimics renal fibrosis, its translatability to human CKD is a limitation. Since CKD arises from diverse causes like diabetes and hypertension, validating our findings in human CKD samples and other CKD models (e.g., adenine-induced, UUO models) is essential. Investigating urinary polyamine levels as potential biomarkers and assessing polyamine-targeted therapies in preclinical humanized models may further enhance clinical relevance.

In summary, our study demonstrated that disruption of polyamine metabolism distribution, particularly through the spermidine/spermine axis, contributes to renal fibrosis and CKD progression after AKI. The altered distribution of spermine and spermidine in diseased kidneys highlights the potential of polyamine-targeted precision interventions to mitigate renal fibrosis and preserve kidney function.

CRediT authorship contribution statement

Cheng Xue: Writing – review & editing, Writing – original draft, Validation, Investigation, Funding acquisition, Conceptualization. **Jiaxin Chen:** Writing – original draft, Validation, Investigation, Conceptualization. **Xinming Li:** Writing – review & editing, Validation, Investigation. **Chenchen Zhou:** Writing – review & editing, Validation, Investigation. **Zhiguo Mao:** Writing – review & editing, Validation, Investigation, Funding acquisition, Conceptualization.

Funding

This work was supported by grants from the National Natural Science Foundation of China (82200786, 82070705, 81770670, and 81873595). This work was supported by Oriental Talent Plan Outstanding Program 2023, Shanghai Municipal Key Clinical Specialty (shslczdzk02503), Shanghai Science and Technology Talent Program (19YF1450300), and Research Projects of Shanghai Science and Technology Committee (17411972100). Shanghai Shenkang Research Physician innovation and transformation ability training program SHDC2022CRD024. Shanghai Science and Technology Innovation Action Plan of Scientific Instruments and Chemical Reagents Project (24142201800), and China Scholarship Council (202408310237).

Declaration of competing interest

The authors declare that they have no known competing financial interests or personal relationships that could have appeared to influence the work reported in this paper.

Acknowledgments

This work was supported by grants from the National Natural Science Foundation of China (82200786, 82070705, 81770670, and 81873595). Oriental Talent Plan Outstanding Program 2023, Shanghai Municipal Key Clinical Specialty (shslczdzk02503), Shanghai Science and Technology Talent Program (19YF1450300), and Research Projects of Shanghai Science and Technology Committee (17411972100). Shanghai Shenkang Research Physician innovation and transformation ability training program SHDC2022CRD024. Scientific and technological innovation action plan of Shanghai medical innovation research 22Y11905500 special project. Shanghai Science and Technology Innovation Action Plan of Scientific Instruments and Chemical Reagents Project (24142201800), China Scholarship Council (202408310237).

Appendix A. Supplementary data

Supplementary data to this article can be found online at https://doi.org/10.1016/j.bbrep.2025.101967.

Data availability

Data will be made available on request.

References

[1] T.K. Chen, D.H. Knicely, M.E. Grams, Chronic kidney disease diagnosis and management: a review, JAMA, J. Am. Med. Assoc. 322 (2019) 1294–1304.

[2] W. Han, C. Du, Y. Zhu, et al., Targeting myocardial mitochondria-STING-polyamine Axis prevents cardiac hypertrophy in chronic kidney disease, JACC Basic Transl Sci 7 (2022) 820–840.

[3] M. Amin, S. Tang, L. Shalamanova, et al., Polyamine biomarkers as indicators of human disease, Biomarkers 26 (2021) 77–94.

[4] D. Luo, X. Lu, H. Li, et al., The spermine oxidase/spermine Axis coordinates ATG5-mediated autophagy to orchestrate renal senescence and fibrosis, Adv. Sci. (2024) e2306912.

[5] S. Mandal, A. Mandal, H.E. Johansson, et al., Depletion of cellular polyamines, spermidine and spermine, causes a total arrest in translation and growth in mammalian cells, P Natl Acad Sci Usa 110 (2013) 2169–2174.

[6] K. Igarashi, S. Ueda, K. Yoshida, et al., Polyamines in renal failure, Amino Acids 31 (2006) 477–483.

[7] S. Bettuzzi, M. Marinelli, P. Strocchi, et al., Different localization of spermidine/spermine N1-acetyltransferase and ornithine decarboxylase transcripts in the rat kidney, FEBS Lett. 377 (1995) 321–324.

[8] D. Luo, X. Lu, Y. Li, et al., Metabolism of polyamines and kidney disease: a promising therapeutic target, Kidney Dis. 9 (2023) 469–484.

[9] Z. Wang, K. Zahedi, S. Barone, et al., Overexpression of SSAT in kidney cells recapitulates various phenotypic aspects of kidney ischemia-reperfusion injury, J. Am. Soc. Nephrol. 15 (2004) 1844–1852.

[10] A. Doğan, A.M. Rao, J. Hatcher, et al., Effects of MDL 72527, a specific inhibitor of polyamine oxidase, on brain edema, ischemic injury volume, and tissue polyamine levels in rats after temporary middle cerebral artery occlusion, J. Neurochem. 72 (1999) 765–770.